Characterization of a dithiol probe for fluorescence-based thiol detection

Natalia Bodnar[1], Robert D. Bongard[1], Fong Yang[1], Phani K. Puella[2], Said H. Audi[3,4,5,6], Ekhson Holmuhamedov[7], and Daniel S. Sem[1*]

[1]School of Pharmacy, Concordia University Wisconsin, Center for Structure-based Drug Design & Development, Mequon, WI, 53097, USA, [2]CMR Institute of Technology, Bangalore-37, India, [3]Dept. of Biomedical Engineering, Marquette University, Milwaukee, WI, 53233, USA, [4]Zablocki VA Medical Center, Milwaukee, WI, 53295, USA, [5]Division of Pulmonary and Critical Care Medicine, Medical College of Wisconsin, Milwaukee, WI, 53226, USA, [6]Dept. of Biomedical Engineering, Medical College of Wisconsin, Milwaukee, WI, 53226, USA, [7]Aurora Research Institute, Aurora Health Care, Milwaukee, WI, 53215, USA. Correspondence should be addressed to D.S.S. (daniel.sem@cuw.edu).

Overview

Purpose: Determine thiol reactivity, reduction potential, and membrane permeability of a dithiol-linked probe (DSSQ), exhibiting fluorescence resonance energy transfer (FRET) quenching in its oxidized form (Fig. 2).

Methods: Fluorescence intensity in the presence of reduced glutathione was used to quantify probe reactivity and reduction potential, confocal fluorescence microscopy and fluorescence intensity measurements of DSSQ-treated cells were used to detect membrane permeability.

Results: DSSQ reacted with GSH in a pseudo first order reaction, probe reduction potential (-0.50 V) suggests minimal impact on intracellular thiol levels, and confocal fluorescence microscopy revealed DSSQ membrane permeability.

Introduction

- Several pathophysiological events are associated with oxidative stress, often with a concomitant change in intracellular thiol redox state.
- A probe capable of dynamic monitoring of cellular thiol levels would be a useful marker for identification of oxidative stress in high content screening.
- Such a probe needs to be thiol-reactive, cell membrane permeable, and have a low reduction potential so as not to oxidatively stress the cell.
- Herein we report the synthesis and characterization of a novel dithio tethered probe (DSSQ) based on fluorescein and p-methyl red and begin to characterize probe thiol reactivity, reduction potential and permeability, including a computational model descriptive of probe-thiol reaction kinetics.

Methods

DSSQ synthesis, two step procedure

Step 1: p-methyl red-cystamine amine monomer synthesis

Step 2: amine monomer + fluorescein isothiocyanate conjugation yielding the final product, DSSQ

Purification; Characterization by 1H NMR, [1H,1H] COSY and MALDI-TOF mass spectrometry

In vitro reaction kinetics of DSSQ with GSH

Fluorescence intensity measurements of buffer samples containing 5 μM DSSQ and 0 – 128 mM GSH were collected at Ex525/Em485 every two minutes for 180 min. Reaction kinetics of fluorescence emission intensity (F) as a function of time (t) were fitted to: $F = F_0 + \Delta F\left(1 - e^{-kt}\right)$, ***equation 1*** where $\Delta F = F_{eq} - F_0$, the recorded fluorescence change, F_{eq} is the fluorescence value at equilibrium (completed reaction), and k is the rate constant for the reaction between GSH and DSSQ at a given concentration of GSH. All kinetic studies were performed at pH 7.0 and 25°C.

Determination of DSSQ reduction potential

DSSQ reduction potential was determined over a range of GSH concentrations as: $E^{o\prime}_{DSSQ} = E^{o\prime}_{GSH} + \left(\frac{RT}{nF}\right) log\left(K_{eq}\right)$, ***equation 2***, where $E^{o\prime}_{GSH}$ = -0.24 V, n = 2, and K_{eq} the equilibrium constant, determined from kinetic study F_{eq} values.

Demonstration of DSSQ cell membrane permeability

Eukaryotic cell studies. NIH 3T3 mouse embryonic fibroblast cells were incubated with Hoechst (1μg/mL), TMRM (0.2 μM), and DSSQ (20 μM) for 30 min. at 37°C to image nuclei, mitochondria, and intracellular thiols, respectively, with or without pretreatment with 10 mM N-acetylcysteine, a cell permeant thiol. Washed cells were imaged with an Olympus Fluoview FV1000 confocal laser scanning microscope using 405 nm, 559 nm and 488 nm lasers to image Hoechst, TMRM, and DSSQ, respectively.

Bacterial cell studies. Equal densities of *E. coli* BL21 DE3 strain and Origami strain, having mutations for thioredoxin B and glutathione reductase were incubated in buffer containing 10 – 50 μM DSSQ. Cells were then washed and resuspended in fresh buffer, placed in fluorescence cuvettes and fluorescence emission intensity spectra recorded between 495-600 nm (excitation 485 nm) at timed intervals over 120 min.

DSSQ protein binding: fluorescence polarization

DSSQ (1 and 5 μM) in 100 mM HEPES buffer pH 7.0, 25°C was titrated with 0 – 250 μM bovine serum albumin (BSA). Parallel and perpendicular fluorescence emission intensity was measured at Em525/Ex485. Fluorescence polarization (FP) was calculated as:

$FP = \frac{(F_{parallel} - F_{perpendicular})}{(F_{parallel} + F_{perpendicular})}$, ***equation 3,*** and plotted as a function BSA concentration. Nonlinear model fits to the data were used to determine the equilibrium dissociation constant K_d, descriptive of binding affinity.

Computational model development

A mathematical model of DSSQ – GSH reactivity was developed to begin to quantify the qualitative features of the dose response kinetic data and evaluate and model the contributing mechanisms.

Results

DSSQ probe chemical structure

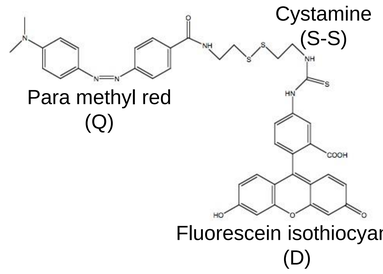

Fig. 1. DSSQ chemical structure. DSSQ synthesis involved tethering a fluorescein donor (D) to a para methyl red quencher (Q) using an aliphatic dithiol cystamine linker (S-S). An aromatic linker version was also prepared.

Thiol detection: DSSQ mechanism of action

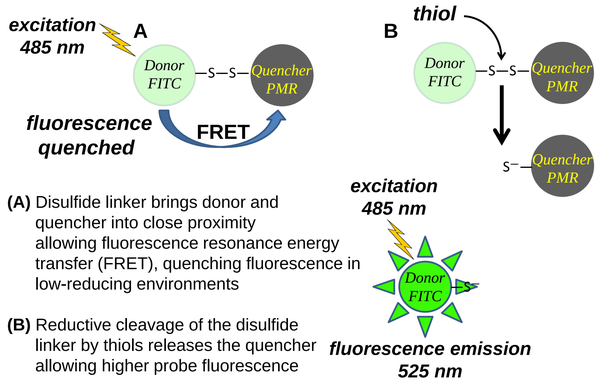

(A) Disulfide linker brings donor and quencher into close proximity allowing fluorescence resonance energy transfer (FRET), quenching fluorescence in low-reducing environments

(B) Reductive cleavage of the disulfide linker by thiols releases the quencher allowing higher probe fluorescence

Fig. 2. Proposed reaction mechanism for thiol detection by DSSQ.

In vitro DSSQ reactivity with GSH

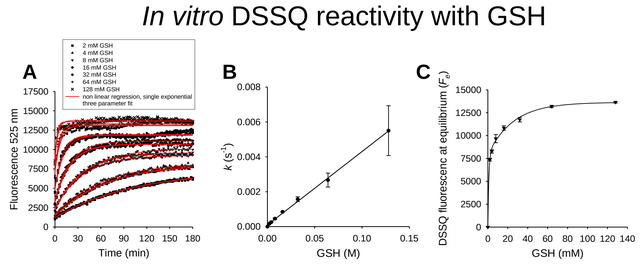

Fig. 3. (**A**) DSSQ (5 μM) fluorescence intensity in the presence of GSH (2 – 128 mM) was monitored for 180 min. Reaction progress curves were fitted (red line) to ***equation 1*** (methods) yielding rate constants k, and equilibrium fluorescence intensity values for each GSH concentration. (**B**) Reaction rate constants plotted as a function of [GSH] revealed that k was pseudo first order in [GSH]. (**C**) Reaction plateau fluorescence intensity plotted as a function of [GSH] showed 5 μM DSSQ was not fully reduced at *in vitro* [GSH] from 2-64 mM, indicating that probe fluorescence would respond to physiologically relevant changes in GSH levels, such as from 5-50 mM, at pH 7.0.

Table 1. DSSQ equilibrium fluorescence intensity (F_{eq}), equilibrium constants (K_{eq}), and DSSQ reduction potentials $(E^{o\prime}_{DSSQ})$ determined over a range of GSH concentrations. $E^{o\prime}_{DSSQ}$ was calculated using ***equation 2*** (methods).

	GSH					
	2 mm	4 mM	8 mM	16 mM	32 mM	68 mM
F_e	7,396 ± 153	8,268 ± 181	9,673 ± 446	10,833 ± 225	11,737 ± 248	13,177 ± 129
K_{eq}	1.80 ± 0.15 x 10^{-9}	1.41 ± 0.12 x 10^{-9}	1.35 ± 0.28 x 10^{-9}	1.12 ± 0.12 x 10^{-9}	8.34 ± 0.90 x 10^{-10}	8.10 ± 0.52 x 10^{-10}
$E^{o\prime}_{DSSQ}$ (V)	-0.499 ± 0.001	-0.502 ± 0.001	-0.503 ± 0.002	-0.505 ± 0.002	-0.509 ± 0.001	-0.509 ± 0.001

DSSQ protein binding

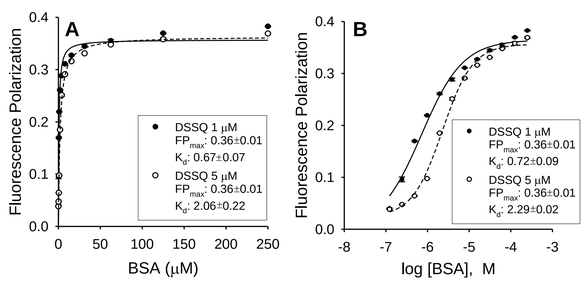

Fig. 4. DSSQ protein binding affinity was determined by fluorescence polarization (FP). DSSQ fluorescence polarization was calculated using ***equation 3*** (methods) and plotted (**A**) as a function of [BSA] or (**B**) as a function of log[BSA]. Data were fitted using nonlinear regression models yielding values for FP_{max}, maximum FP, and K_d, the dissociation constant reflective of binding affinity. Apparent K_d decreases with decreasing BSA, consistent with stoichiometric covalent binding of probe. Maximum polarization of 360 mP is consistent with a highly immobilized probe, once bound.

DSSQ membrane permeability

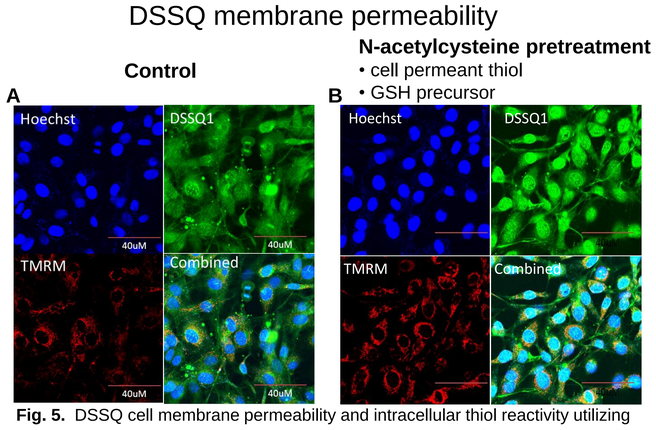

Fig. 5. DSSQ cell membrane permeability and intracellular thiol reactivity utilizing NIH 3T3 mouse embryonic fibroblasts. (**A**) Cells were pretreated with buffer or (**B**) 10 mM NAC (to increase intracellular thiol levels) for 30 min. at 37°C, washed with buffer, then incubated with Hoechst, TMRM, and DSSQ to image nuclei, mitochondria, and intracellular thiols, respectively. The reagents were removed and the cells washed three times before image collection by confocal laser microscopy.

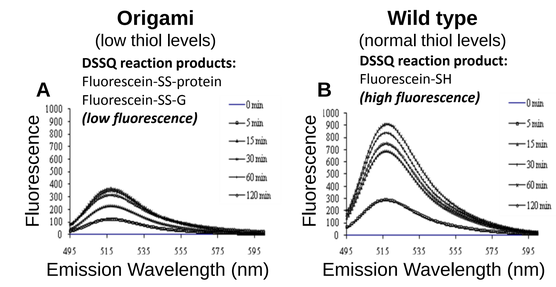

Fig. 6. Relative thiol/disulfide levels in bacteria. (**A**) Origami and (**B**) wild type *E. coli* were incubated with DSSQ, washed, and resuspended in buffer, and fluorescence intensity spectra collected over 120 min. The higher fluorescence intensity observed in the wild type samples suggests DSSQ membrane permeability and sensitivity to intracellular thiol levels.

Computational model for DSSQ reactivity with GSH

Assumed reactions

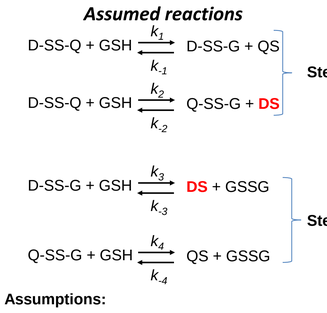

Governing differential equations

$$\frac{d[D-SS-Q]}{dt} = \alpha\left(-k_1[D-SS-Q][GSH] + k_{-1}[QS][D-SS-G]\right) + (1-\alpha)\left(-k_2[D-SS-Q][GSH] + k_{-2}[DS][Q-SS-G]\right)$$

$$\frac{d[D-SS-G]}{dt} = \alpha\left(k_1[D-SS-Q][GSH] - k_{-1}[QS][D-SS-G]\right) - k_3[D-SS-G][GSH] + k_{-3}[DS][GSSG]$$

$$\frac{d[Q-SS-G]}{dt} = (1-\alpha)\left(k_2[D-SS-Q][GSH] - k_{-2}[DS][Q-SS-G]\right) - k_4[Q-SS-G][GSH] + k_{-4}[QS][GSSG]$$

$$\frac{d[QS]}{dt} = \alpha\left(k_1[D-SS-Q][GSH] - k_{-1}[QS][D-SS-G]\right) + k_4[Q-SS-G][GSH] - k_{-4}[QS][GSSG]$$

$$\frac{d[DS]}{dt} = (1-\alpha)\left(k_2[D-SS-Q][GSH] - k_{-2}[DS][Q-SS-G]\right) + k_3[D-SS-G][GSH] - k_{-3}[DS][GSSG]$$

$$\frac{d[GSSG]}{dt} = k_3[D-SS-G][GSH] - k_{-3}[DS][GSSG] + k_4[Q-SS-G][GSH] - k_{-4}[QS][GSSG]$$

$[D\text{-}SS\text{-}Q](t=0) = [D\text{-}SS\text{-}Q](t) + [D\text{-}SS\text{-}G](t) + [Q\text{-}SS\text{-}G](t) + [GSSG](t)$
$= [D\text{-}SS\text{-}Q](t) + [Q\text{-}SS\text{-}G](t) + [QS](t)$
$= [D\text{-}SS\text{-}Q](t) + [D\text{-}SS\text{-}G](t) + [DS](t)$

$[QS](t) = [D\text{-}SS\text{-}G](t) + [GSSG](t)$
$[DS](t) = [D\text{-}SS\text{-}G](t) + [GSSG](t)$

Assumptions:

- α = fraction of step 1 that results in D-SS-G + QS due to attack at the thiol proximal to the fluorescein (vs. PMR thiol)
- GSH = concentration in excess and hence assumed constant
- DS = fluorescein half of the probe, as the only fluorescent species (assumes DS-SG is not fluorescent)

Model Simulations

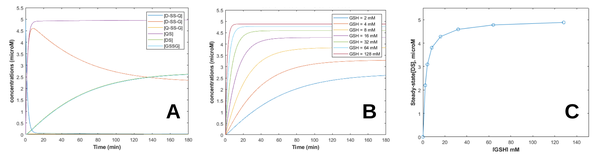

Rate Constant ($mM^{-1}min^{-1}$)	
k^1	5.0×10^{-4}
k^{-1}	2.5×10^{-3}
k^2	2.5×10^{-6}
k^{-2}	2.5×10^{-3}
k^3	4.0×10^{-6}
k^{-3}	2.5×10^{-3}
k^4	4.0×10^{-6}
k^{-4}	2.5×10^{-3}

Fig. 7. Computational model simulations for (**A**) the different species of DSSQ present in the reaction as a function of time with [DSSQ] = 5 μM, [GSH] = 2 mM, and [GSSG] = 0 μM at t = 0, (**B**) the time course of DSSQ reduction to DS^- over a range of GSH concentrations (data from Fig. 3A), and (**C**) steady state DS^- concentrations as a function of [GSH] (data from Fig. 3C), (**D**) model simulation rate constants at α = 0.5 (manual optimization); may differ from those that best fit the model solution to the data.

Conclusions

DSSQ is a cell permeant probe (both Eukaryotic and Prokaryotic) that is responsive to changes in GSH concentrations in a physiologically relevant range, from 5-50 mM.

The low reduction potential of the DSSQ probe (-0.50 V) indicates it will not deplete intracellular thiols, thereby causing oxidative stress.

Changes in real time intracellular thiol levels can be monitored by changes in the equilibrium fluorescence emission by the probe.

Because of the above properties, the probe can be used for screening and imaging oxidative stress is cells, in high content screening assays.

References

Puella, P.K., Chiku, T., Carvan, M.J. III, and Sem, D.S. Fluorescence-based detection of thiols *in vitro* and *in vivo* using dithiol probes. *Anal. Biochem.* **352**, 265-273 (2006).

Yang, F., Godic, Z, Negmadjanov, U., and Sem, D, and Holmuhamedov, E. A novel SH-sensing fluorescent probe to monitor the redox status of intracellular compartments. J. Patient-Centered Res. Rev. **1**, 149-50 (2014).